Reports

Stereoscopic Images in Confocal (Tandem Scanning) Microscopy

Abstract. *Stereoscopic pair images with parallel projection geometry are obtained by through-focusing along two inclined axes while recording two (summed and stacked) images with a microscope with a very shallow depth of field. The two stack images sample the same depth slice of translucent or reflective specimens. The method will work most conveniently with a tandem scanning microscope (a direct-view, confocal scanning optical microscope). This is a direct method for recording stereo images that can be used to the limit of resolution in optical microscopy. It demonstrates a previously unrealized advantage of confocal optical microscopy.*

ALAN BOYDE
Department of Anatomy and Embryology, University College London, Gower Street, London WC1E 6BT England

Man has an extremely well-developed sense of distance perception based upon stereoscopic vision. However, in spite of the long period of development of light microscopy, we still have no satisfactory, simple means for the recording of images which both preserve the structural information contained in the specimen layer and can be viewed stereoscopically to obtain a three-dimensional (3D) impression at high resolution.

Direct stereoscopic viewing at high resolution in a conventional light microscope is not possible for several reasons. (i) Increasing the objective aperture to improve the resolving power reduces the depth of field. (ii) Lateral resolution is spoiled by a thick sample as a result of high-contrast features in out-of-focus layers. To obtain the highest (lateral) resolution, therefore, it is the usual practice to use thin objects, but in so doing all the information from the other specimen layers in depth is removed. (iii) Even if not object limited, light microscopy would be limited by the reduction in depth of field with improving lateral resolution, so that in the extreme case of optimum resolving power, the layer from which the information is derived again has so little depth that there is little "third dimension" to appreciate.

A general solution to the above problems is, paradoxically, to start by reducing the depth of field of the optical microscope to the maximum extent, since by doing so out-of-focus images of high-signal features that usually contaminate the image of a thick object space can be avoided. The means for doing this is provided by the confocal scanning, point-source, point-illumination, point-detector microscopes (*1–6*), which improve both contrast and resolution in *X–Y* and *Z*. In one type, the specimen is scanned mechanically in a raster past a stationary optical beam of laser origin, the image being reconstructed on a TV display (*1–4*). In another type (*5, 6*), the multiple sources, illuminating patches, and detectors are achieved by the use of a single, complex aperture wheel, and a direct view, real-time, real-color image is obtained of the whole field of view. This latter type of confocal or tandem scanning microscope should make the development described here the more easily achieved. However, the prime requirement is a confocal scanning optical microscope (*1–10*).

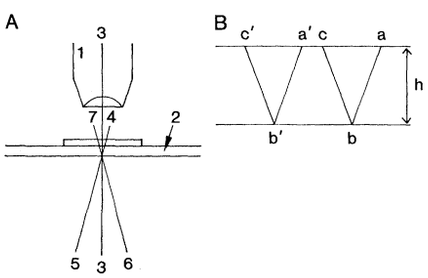

Fig. 1. Diagrams explaining means for acquiring stereo-pair images with the tandem scanning reflected light microscope (*9, 10*). (A) 1, objective lens; 2, specimen, shown as a slide with cover slip (but it can be any object); 3–3, optic axis, which is the focusing axis in conventional microscopy; 4–5, axis for through-focusing to give the right eye view; 6–7, axis for through-focusing to give the left eye view in the stereo pair. (B) *h*, thickness of the stereo slice to be imaged; *a′a*, two points in the upper plane of the stereo slice; *b′b*, two points in the lower plane of the stereo slice that are overlapped by *a′a* in the right eye view [gained by focusing along 4–5 in (A)]; *c′c*, two points in the upper plane that overlap *b′b* in the left eye projection [through-focusing along 6–7 or 7–6 in (A)].

The tandem scanning microscope is an optical sectioning microscope: one can study 3D structure by focusing up and down and interpreting the coming and going of features and their relative shifts. By recording a sequence of images, usually at a regular series of intervals, it is possible to make a formal reconstruction of the object space that has been photographed (*7, 8*). The sequence of "optical sections" is printed on plates (or films) that are stacked at the proper interval, so that a 3D model is formed in this stack. Such images can alternatively be recorded in frame store, computer memory, or video disk or tape and processed by computer (*4*).

Stereo pair images of a stack of photographs are obtained in one of two ways. The stack is shifted in contact printing so that the rays of light that pass through the stack do so with differing, opposing obliquities, corresponding to left and right eye views through the stack. Alternatively, the stack is sheared between the two exposures so that every optical section is shifted by a small amount relative to its neighbor (*8*).

The tedium of recording, processing, stacking, and registering the component images of a stack and of discovering the correct optical density for the image of each layer so as to avoid peak white or black in feature overlaps can be simply overcome by recording each stack as one composite image in first instance. In the simplest and most economical case, the two stack images are recorded on photographic emulsion, but it makes no difference whether other means of image storage are employed (such as videotape, video disc, or frame store) or whether these are the final or the intermediate means of image recording or display.

As a practical means of acquiring stereo images by this method, I have used a direct view, tandem scanning optical microscope from Petran and Hadravsky (*5, 6, 9*). The specimen is moved vertically with respect to the objective during each of the two photographic exposures, but at the same time it is slewed sideways in the direction of the interocular axis for viewing the completed stereo pair. Both members of the stereo pair sample the same object depth (*h*, Fig. 1B), and both are perfect parallel projection images of this layer. Lateral shift need only occur during one of the exposures, one axis of view being normal to the sampled slice volume. The more usual system would be to employ two equal and opposite lateral shifts (slews) so that the mean

stereo viewing axis was normal to the plane of the slice within the object. However, it would also be possible to use two slews of the same sense but different velocity to obtain an oblique stereo view through the object space.

An example of the procedure is illustrated by Fig. 1, A and B. A mechanical stage moving the specimen or the objective or the microscope in the direction of 4–5 in Fig. 1A is activated at the same time that a photographic exposure is commenced. Movement along 4–5 occurs while the plane of focus changes from *a–a'* to *b–b'* (Fig. 1B) when the photographic exposure is stopped. A second photograph corresponding to the view of the second eye in stereo viewing begins at level *b–b'*, with the movement along 6–7 activated. During this exposure, the sample moves such that features at level *b–b'* at the beginning overlap *c–c'* at the completion of the exposure.

This approach provides a simple means of photographing translucent specimens to obtain stereoscopic views from which 3D aspects of internal structure can be appreciated. With this method, 3D imaging of thick optical sections can be obtained by simple and direct means, potentially close to the limit of resolution of light microscopy. Since this method would obviously be best employed with a tandem scanning, direct-view, confocal microscope, and since these microscopes are expected to show improvement in resolution beyond the limit of the conventional optical microscope (0.61λ divided by numerical aperture) already shown for the unitary beam instruments (*2–4*, *10*), the method may also eventually exceed the resolution limits of conventional optical microscopy.

The basic means for recording stereo images described here can be employed in any optical microscope, but there are strong advantages of the confocal types stemming from the improvements in contrast, lateral resolution, and depth resolution. A further advantage of the confocal scanning optical microscopes is that they can be used to select precisely the depth within the object and the total thickness of the layer to be reconstructed by stereo imaging. This choice can be performed by simple, direct inspection of the image in the tandem scanning microscope (*5–9*).

This method will be limited mainly by the characteristics of real objects and real objective lenses. Thus the translucency of the object will be impaired in proportion to the frequency of the light-influencing features that are being visualized, except in the case of a weakly scattering fluorescent sample. Further, objectives with high resolving power have a short free-working distance. However, the stereo images obtained by this method have parallel projection geometry, which is much simpler than perspective projection, and simple, reliable stereophotogrammetric instruments developed for work in scanning electron microscopy in this laboratory are thus available and suitable for analysis of the images (*11*, *12*).

Studies conducted so far that have demonstrated the feasibility of this system (Figs. 2 to 4) have also shown that the stereo images have the further advantage of "removing" the scanning lines resulting from imperfections in the manufacture of the Petran-Hadravsky aperture disk to a perceived plane distinct from the layer in which the appar-

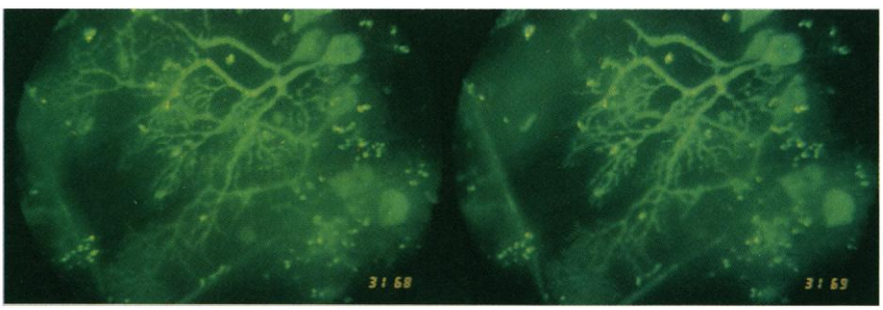

Fig. 2. Forty-micrometer stereo slice in a 90-μm thick section of mouse cerebellum, Golgi-Cox stained; 50/0.95 oil objective, 14° stereo angle. Original on Ektachrome 400 color transparency film (preparation by M. Berry).

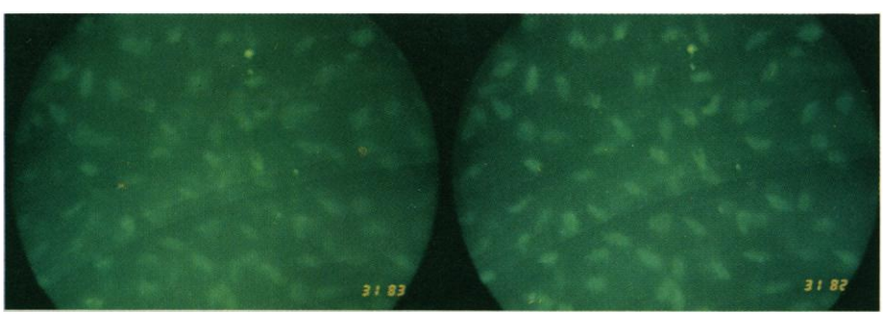

Fig. 3. *Hemigalago* (bush baby) parietal bone (30-μm stereo slice deep to external surface of entire skull; 50/0.95 oil objective, 14° stereo angle. Original on Ektachrome 400 color transparency film.

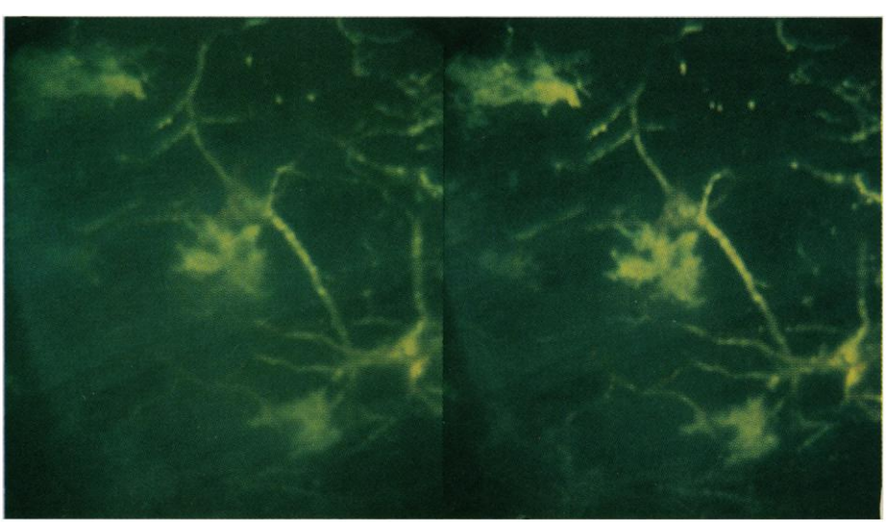

Fig. 4. Fifty-micrometer stereo slice in a 90-μm thick section of rat spinal cord, L4–L5 level, Golgi stain; 40/0.85 oil objective, 10° stereo angle. Original on Ektachrome 400 transparency film (preparation by J. E. Swett).

ent 3D image plane lies. With the geometry shown in Fig. 1, A and B, the scanning lines would be seen to lie at level *b–b'*. They can easily be placed outside the apparent volume in which the 3D optical model lies by overlapping the stack images in a plane outside that volume.

Regarding potential areas of application, this method may be useful where 3D interrelations are too difficult to comprehend by simple through-focusing, where analysis by tracing in serial sections or by camera lucida drawing may be too time consuming (as in the study of sections of central nervous system tissue; Figs. 2 and 4), or where serial sectioning or grinding is not allowed because the intrinsic or scientific value of the specimen is too high (as in the study of archaeological jewels or fossils).

References and Notes

1. M. Minsky, U.S. patent 3013467 (1961).
2. T. Wilson, *Scanning* **7**, 79 (1985).
3. _____ and C. J. R. Sheppard, *Theory and Practice of Scanning Optical Microscopy* (Academic Press, London, 1984).
4. H. T. M. van der Voort *et al.*, *Scanning* **7**, 66 (1985).
5. M. D. Egger and M. Petran, *Science* **157**, 305 (1967).
6. M. Petran, M. Hadravsky, M. D. Egger, R. Galambos, *J. Opt. Soc. Am.* **58**, 661 (1968).
7. A. Boyde and S. A. Reid, *Bone*, in press.
8. A. Boyde, *Proc. R. Microsc. Soc.* **20**, 131 (1985).
9. M. Petran, M. Hadravsky, A. Boyde, *Scanning* **7**, 97 (1985).
10. R. W. Wijnaendts van Resandt *et al.*, *J. Microsc.* **138**, 29 (1985).
11. A. Boyde and H. F. Ross, *Photogramm. Rec.* **8**, 408 (1975).
12. P. G. T. Howell and A. Boyde, in *Analysis of Organic and Biological Surfaces*, P. Echlin, Ed. (Wiley, New York, 1984), pp. 325–349.

13. I thank the Medical Research Council (United Kingdom) for support and R. Radcliffe and E. Maconnachie for technical and photographic assistance.

2 August 1985; accepted 4 October 1985

Lattice Images of Solid Xenon Precipitates in Aluminum at Room Temperature

Abstract. *Small solid precipitates (bubbles) of xenon in an aluminum matrix have been formed by ion implantation. Lattice images of this room-temperature inert gas solid were obtained using high-resolution phase-contrast electron microscopy. Many bubbles showed a high degree of crystalline perfection, but regions of defective crystallinity were observed in several cases.*

STEPHEN E. DONNELLY
CHRISTOPHER J. ROSSOUW
Division of Chemical Physics, Commonwealth Scientific and Industrial Research Organisation, Clayton, Victoria 3168, Australia

Since the first recognized solidification of argon in 1895 (*1*), inert gas solids have been the object of many experimental and theoretical investigations. Indeed, their simplicity, from the theoretician's point of view, has rendered inert gas solids a useful testing ground for various aspects of solid-state theory (*2*). Because cryogenic or high-pressure techniques (or both) are required to solidify the gases, high-resolution electron microscopy has not hitherto been applied to the rare gas solids. Recently, Templier (*3*, *4*) and vom Felde (*5*) and their colleagues have used electron diffraction patterns to identify small solid precipitates of xenon and argon at room temperature in ion-implanted aluminum, and Evans and Mazey (*6*) have made a similar observation of solid krypton in a number of metals.

The identification of these precipitates from clearly identifiable (though weak) diffracted beams suggested to us the possibility of performing high-resolution phase-contrast electron microscopy to produce lattice images of the implanted inert gas precipitates. We now present lattice images of solid xenon precipitates in aluminum at room temperature that show regions of both perfect and defective crystallinity. These lattice images of an inert gas solid demonstrate the potential of the "bubble" as a high-pressure cell for electron microscopy and other studies of rare gas solids. In common with other investigators we continue to use the word "bubbles" to describe inert gas precipitates.

Aluminum films approximately 50 nm thick were prepared by evaporation of aluminum in vacuum onto an air-cleaved {100} NaCl surface heated to about 490 K. This procedure resulted in a polycrystalline film containing grains with preferred <100>, <110>, and <111> orientations. Xenon implantation was carried out with 50-keV Xe^+ ions at a flux of approximately 3×10^{16} ion m^{-2} sec^{-1} to a fluence of 10^{20} ion m^{-2}. The films were irradiated on the NaCl substrates at a temperature of 270 ± 10 K. The projected range of these ions was calculated from an analytical model (*7*) to be 25 ± 4 nm. The sputtering yield (*8*) was such that about 15 nm of aluminum was removed during irradiation. The films were floated off the substrate in distilled water and caught on 400-mesh copper grids. The films were then examined at 200 keV using the high-resolution top-entry stage of a transmission electron microscope (JEOL 200 CX).

Figure 1A shows a diffraction pattern from a <110> grain. As in previous diffraction studies (*3–6*), the diffraction pattern has extra reflections, indicating the presence of epitaxial face-centered cubic (*fcc*) precipitates. These represent spacings that are 1.49 ± 0.01 times the aluminum spacing, consistent with an *fcc* lattice parameter of 0.604 ± 0.04 nm. Dark-field microscopy with the extra reflections confirmed that these beams were excited within the implanted bubbles. Although xenon atoms scatter electrons far more strongly than do aluminum atoms, the atomic density in the xenon bubbles was comparatively low, so that the forward scattering potential for electrons in the aluminum matrix was

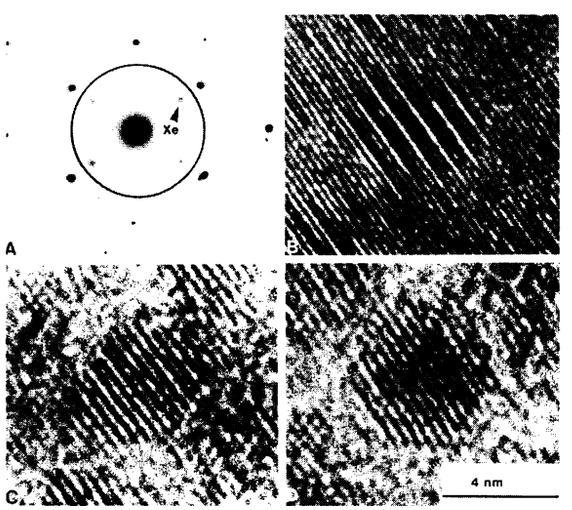

Fig. 1. (A) Diffraction pattern from a <110> aluminum grain. The arrow indicates one of the comparatively weak xenon {111} spots; the circle indicates the size of the 20-μm objective aperture. This aperture excludes the beams diffracted from aluminum from contributing to the image. (B) An image taken with the 50-μm objective aperture, with 0.23-nm {111} aluminum fringes merging with a xenon bubble. Here parallel moiré fringes are evident as an increase in intensity every third fringe spacing. (C) An image taken with a 20-μm objective aperture showing 0.35-nm fringes from {111} xenon planes. (D) An image taken under conditions similar to those for (C), with a defect region in the center of the bubble. Again the fringes are from {111} xenon planes. The scale marker is 4 nm.